Journal of Neuroscience Methods 416 (2025) 110381

Contents lists available at ScienceDirect

Journal of Neuroscience Methods

journal homepage: www.elsevier.com/locate/jneumeth

Ramp protocol for non-linear cerebrovascular reactivity with transcranial doppler ultrasound

Genevieve Hayes *, Sierra Sparks, Joana Pinto, Daniel P. Bulte

IBME, Department of Engineering Science, University of Oxford, Oxford UK

ARTICLE INFO

Keywords:
Cerebrovascular reactivity
Cerebral blood flow
Transcranial Doppler ultrasound
Hypercapnia
Bayesian modeling
Non-linear modelling
Gas stimuli

ABSTRACT

Background: Cerebrovascular reactivity (CVR) reflects the ability of cerebral blood vessels to adjust their diameter in response to vasoactive stimuli, which is crucial for maintaining brain health. Traditional CVR assessments commonly use a two-point measurement, assuming a linear relationship between cerebral blood flow (CBF) and arterial CO_2. However, this approach fails to capture non-linear characteristics, particularly the plateaus at extreme CO_2 levels.

New method: This study introduces a cost-effective, ramp-based end-tidal CO_2 ($PETCO_2$) protocol to assess non-linear aspects of CVR. Using transcranial Doppler ultrasound, we monitored blood velocity responses to progressive increases in arterial CO_2 levels in eleven healthy adults, covering a spectrum from hypocapnia to hypercapnia.

Results: All eleven participants successfully completed the protocol, with an average $PETCO_2$ range of 26 ± 4 mmHg and blood velocity changes from -29 % to $+ 50$ % relative to baseline. Non-linear CVR characteristics were observed in all subjects. Sigmoid models provided significantly better fits to the CVR data than linear models, while Bayesian approaches followed expected physiological ranges more accurately than least squares regression methods.

Comparison with existing methods: Unlike traditional CVR methods, this ramp protocol captures the full, non-linear CVR profile. The sigmoid modeling approach offers a more accurate representation of cerebrovascular dynamics, particularly at CO_2 extremes.

Conclusions: The $PETCO_2$ ramp protocol with non-linear CVR modeling shows promise as an accessible and reliable tool for assessing CBF dynamics. With high completion rates, straightforward implementation, and low equipment cost, this approach holds significant potential for clinical applications in cerebrovascular health evaluation.

1. Introduction

Cerebrovascular reactivity (CVR) describes the capacity for blood vessels in the brain to constrict and dilate in response to vasoactive factors. This metric can be measured by applying a vasoactive stimulus, such as voluntary breathing tasks, gas inhalation protocols, or an acetazolamide injection (Liu et al., 2020; Pinto et al., 2021; Ringelstein et al., 1992), and measuring the concomitant blood flow changes with a non-invasive imaging modality such as magnetic resonance imaging (MRI) or transcranial Doppler ultrasound (TCD).

MRI-based techniques, such as blood-oxygen-level-dependent (BOLD) and arterial spin labelling (ASL) imaging, offer high spatial resolution to non-invasively map CVR (Pinto et al., 2021; Sleight et al., 2021). However, TCD provides a simpler, widely available, and cost-effective alternative, enabling the measurement of blood velocity in major cerebral arteries (Burley et al., 2021; McDonnell et al., 2013).

Hypercapnia induced by inhaling gas mixtures with elevated CO_2 content is a common method to elicit CVR. This increases the partial pressure of arterial CO_2 ($PaCO_2$), typically estimated via end-tidal CO_2 ($PETCO_2$) measurements. While many studies calculate CVR using a two-point approach, one measure at baseline and another during hypercapnia, this method assumes a linear relationship between $PaCO_2$ and cerebral blood flow (CBF) (Sleight et al., 2021; Bright and Murphy, 2013; van der Zande et al., 2005). However, at the end ranges of $PaCO_2$ levels, both hypo- and hypercapnia, the relationship between CO_2 and CBF exhibits non-linear characteristics, often plateauing due to maximal

* Correspondence to: Institute of Biomedical Engineering, University of Oxford, Old Road Campus Research Building, Roosevelt Drive, Oxford OX3 7DQ, UK.
E-mail address: genevieve.hayes@eng.ox.ac.uk (G. Hayes).

https://doi.org/10.1016/j.jneumeth.2025.110381
Received 4 November 2024; Received in revised form 10 January 2025; Accepted 28 January 2025
Available online 28 January 2025

vasoconstriction or vasodilation. This plateau effect indicates that beyond certain CO_2 thresholds, further changes in CO_2 do not elicit corresponding changes in CBF resulting in a non-linear relationship between $PaCO_2$ and blood flow. Progressive changes in CO_2 have indeed demonstrated the sigmoidal nature of CVR in healthy subjects (Battisti-Charbonney et al., 2011; Bhogal et al., 2014; Claassen et al., 2007; Ringelstein et al., 1988).

Existing methods for eliciting and measuring non-linear CVR responses have primarily relied on rebreathing protocols, computerised targeted end-tidal forcing systems, and sequential gas delivery methods. These approaches often involve progressive CO_2 challenges to map CBF responses, leveraging techniques such as TCD or MRI for assessment (Battisti-Charbonney et al., 2011; Bhogal et al., 2014; Claassen et al., 2007; Ringelstein et al., 1988; Fan et al., 2016; Fisher et al., 2017; Sobczyk et al., 2014). While effective, these protocols often require specialized equipment and complex methodologies, limiting their accessibility for broader clinical and research applications. Current non-linear models of CVR commonly utilize a 4-parameter logistic regression to capture physiologically relevant features, such as maximum and minimum CBF responses, the inflection point of CO_2 sensitivity, and the slope in the linear response region (Battisti-Charbonney et al., 2011; Bhogal et al., 2014; Claassen et al., 2007; Fan et al., 2016). Alternative approaches, such as biphasic linear fits or circuit analysis models, have also been applied to delineate CVR response types or vascular bed resistances under progressive CO_2 challenges (Fisher et al., 2017; Duffin et al., 2017). Despite these advances, asymmetric sigmoid models, which may account for differential mechanisms governing cerebral blood vessel dynamics at their smallest and widest calibres, remain unexplored in CVR research.

Motivating our research is the need for more clinically relevant and broadly applicable measures of CVR. The two-point measure, a common surrogate for CVR, fails to capture the complex shape and orientation of the full CVR response, which may limit its diagnostic and therapeutic utility. For example, a shift in baseline CBF reserve or a change in the amplitude or speed of the CVR response could signify distinct pathological mechanisms, yet these nuances remain indistinguishable with a simplified measure. Linear models, while useful, are inherently limited as they rely on a single parameter, slope, to indicate dysfunction. In contrast, non-linear models can account for multiple parameters, such as the inflection point between lower and upper plateaus, the range of the response, and the baseline offset, which may provide deeper insights into the nature of dysfunction and improve our understanding of vascular responses in different pathologies. Given the association of altered CVR with conditions such as stroke, cognitive decline, and traumatic brain injury, advancing our ability to assess these dynamics comprehensively is critical (Churchill et al., 2020; da Costa et al., 2016; Krainik et al., 2005; Markus and Cullinane, 2001; Mutch et al., 2016; Aslanyan et al., 2024). While further research is needed to validate these applications, capturing the full spectrum of CVR dynamics without the need for complex protocols or equipment could ultimately enhance diagnostic precision and support the development of tailored therapeutic strategies.

In our study, we aim to address these limitations by presenting a cost-effective and widely accessible protocol for eliciting non-linear CVR responses using a combination of voluntary breathing techniques and gas stimuli. We measure the resulting CBF changes in the middle cerebral artery (MCA) using TCD, providing a robust and practical approach to characterizing cerebrovascular dynamics. In addition, we evaluate and compare multiple modelling strategies, including 4-parameter (symmetric) and 5-parameter (asymmetric) sigmoidal models, to capture the full spectrum of CVR responses. By incorporating least-squares regression and Bayesian methods, we aim to identify an accurate and clinically relevant approach to modelling CVR.

2. Materials and methods

2.1. Ethical approval

All experimental procedures and protocols were approved by the Medical Sciences Interdivisional Research Ethics Committee (MS IDREC) of the University of Oxford's Central University Research Ethics Committee (CUREC), all of which conformed with the Declaration of Helsinki. Written informed consent was obtained for all participants before taking part in the study.

2.2. Data acquisition

A total of 11 healthy participants (5 female, 33 ± 9 years of age) were included in this study. All participants were non-smokers with no history of psychiatric or brain disorders, hypertension, diabetes, or cardiovascular disease. The sample size of 11 subjects was chosen based on precedent set by similar studies employing non-linear CVR methods, which have typically used sample sizes ranging from 8 to 18 subjects (Battisti-Charbonney et al., 2011; Bhogal et al., 2014, 2015; Claassen et al., 2007; Fisher et al., 2017).

To characterise the dynamics of the cerebral blood flow response to the novel CVR protocol, blood flow velocity in the left MCA was measured continuously using a 2 Hz probe and clinical TCD (7760EN Doppler-BoxX Digital, Compumedics DWL). Along with transmission gel, the TCD probe was placed on the transtemporal window and was secured using an adjustable headset. The location and angle of the probe was changed until a consistent blood flow velocity was achieved with a high signal-to-noise ratio. All TCD data were acquired by a single trained operator to ensure consistency and minimize operator-dependent variability. Signal quality was confirmed qualitatively by the trained operator, ensuring stable, pulsatile waveforms with clear spectral delineation of systole and diastole, and high peak-to-background amplitude.

A thin nasal cannula placed into both nostrils was used to sample CO_2 and O_2 levels in respired air and an infrared gas analyser (ML206, ADInstruments). The CO_2, O_2, and TCD signals were recorded using a PowerLab 8/35, 8 Channel recorder (PL3508 ADInstruments) and accompanying LabChart Software.

Inspired gases were delivered using a custom gas delivery system built in-house at the University of Oxford (Sparks et al., 2024). The setup consisted of a disposable non-rebreathing anaesthetic face mask (Model 1181015, Intersurgical EcoLite Oxygen Mask) placed over the participant's nose and mouth, secured using a head strap. Unidirectional silicon membranes on either side of the mask allowed exhaled air to escape the mask while being sealed during inhalation and a medical-grade respiratory filter (Model 1644007, Clear-Guard Midi Low Volume Breathing Filter) was placed at the junction of the disposable circuit and the permanent fixtures to prevent cross-contamination. On the permanent side of the filter, a short length of tubing attached to two interconnected Y-pieces where respiratory gas mixtures could be delivered one at a time at 15 L/min. The gas cylinders, each fitted with a pressure regulator and flow metres, were operated by hand, following a predefined ramp protocol.

The ramp protocol consisted of 3 repetitions of 5 deep breaths, followed by 30 s of regular breathing on synthetic medical air (21 % O_2 / 79 % N_2), 40 s breathing a 5 % CO_2 balanced gas mixture (BOC Group, Linde, Surrey, UK), and 40 s breathing a 10 % CO_2 balanced gas mixture (BOC Group, Linde, Surrey, UK). A diagram of the protocol is illustrated in Fig. 1. The deep breathing instructions were given verbally and the participants were notified when the gases were changed and for the last 10 s of breathing the 10 % CO_2 gas mixture. Participants were trained prior to starting the ramp protocol to take full deep breaths without pauses and were allowed to test breathing the different gases. This testing time was also used to check for leaks at the mask-face interface identified via the capnometry trace which were plugged with additional

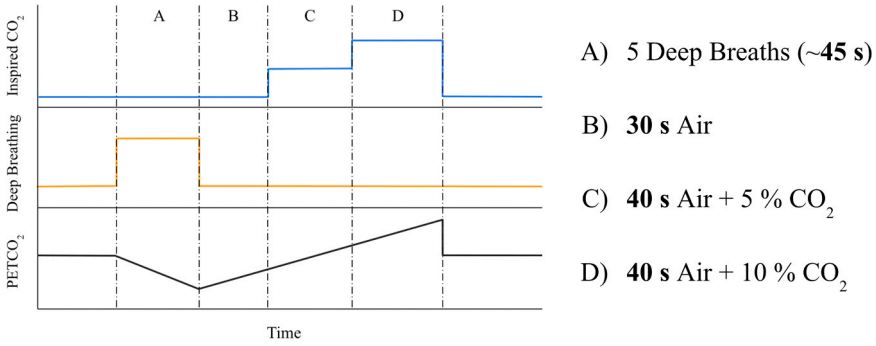

Fig. 1. Ramp paradigm diagram consisting of A) 5 deep breaths, B) 30 s of air, C) 40 s of air with 5 % CO_2, and D) 40 s of air with 10 % CO_2. The full ramp protocol consisted of 3 repeats of this sequence.

rubber fittings if needed.

2.3. Data analysis

2.3.1. Preprocessing

The CO_2, O_2, and TCD data were acquired at 200 Hz. Data processing and analysis was performed using custom scripts in Python 3.10.8. The raw TCD outputs were converted to cm/s using a calibration factor of 202.07 cm/s/V based on the DWL software, and values below 14 cm/s were removed as they corresponded with bottoming out of the TCD signal. The gas signals were converted from percent to mmHg using a conversion factor derived from the acquisition-day 12.00 PM atmospheric pressure in Oxford, UK (EODG).

A rolling mean of the MCA velocity (MCA$\underline{v}$) was applied across the pulsatile signal. The end-tidal peaks in the CO_2 and O_2 time-courses were selected automatically. To account for measurement delay, a bulk shift was applied to each $PETCO_2$ trace to maximise its cross-correlation with the mean MCA$\underline{v}$ signal. To account for equipment and physiological delays, a manual shift (mean across subjects of -16 ± 8 s) was applied to align each participant's $PETCO_2$ trace with their MCA$\underline{v}$ trace. A low-pass filter was applied to the MCA$\underline{v}$ and $PETCO_2$ time courses with a window size of 50 samples, corresponding to a time window of 0.25 s at the sampling rate of 200 Hz, corresponding to an effective cutoff frequency of 2 Hz. The filter was implemented using the rolling mean method in Python's Pandas library, which calculated the rolling average over the specified window size (The pandas development team, 2024). This approach smoothed high-frequency noise while preserving the physiological signal's key characteristics. MCA$\underline{v}$ was normalised relative to the mean MCAv during the baseline period (breathing air) to account for any variations in probe angle relative to the MCA. Only the 3 ramp-up, blood vessel dilation components of the protocol were isolated for further analysis since the dynamics for dilation and constriction may not be the same (Zheng et al., 2010). This approach was chosen to prioritize consistency in the modelling process and reduce potential variability.

2.3.2. Model fitting

CVR was characterised by fitting 4-parameter and 5-parameter sigmoid models to the MCA$\underline{v}$ vs. $PETCO_2$ data for each subject as shown in Eq. (1) and Eq. (2) respectively. In these equations, 'a' represents the minimum blood velocity (bounded between 0 <a<1 a.u.), 'b' represents the slope of the linear region (0 <b<20 mmHg/a.u.), 'c' describes the $PETCO_2$ value for the inflection point (0 <c<60 mmHg), and 'd' is the span of the blood velocity (0 <d<4 a.u.) (Bhogal et al., 2014; Claassen et al., 2007). It should be noted that the inflection point in the sigmoid model represents the CO_2 level corresponding to the steepest slope of the curve, marking the transition between lower and upper plateaus, irrespective of the specific CO_2 inhalation conditions. The 5th parameter in Eq. (2), 's', is an asymmetry parameter that allows the lower and upper plateaus to occur at different rates (0.1 <s < 10 a.u.).

$$y = a + \frac{d}{1 + e^{\frac{(c-x)}{b}}} \tag{1}$$

$$y = a + \left(\frac{d}{1 + e^{\frac{(c-x)}{b}}}\right)^{s} \tag{2}$$

Fitting of these models was done using a least-squares regression (LSR) method with SciPy (Virtanen et al., 2020) and a Bayesian nested sampler method with the python package BayesicFitting (Kester and Mueller, 2021). Gaussian priors were used for the parameters in the Bayesian fitting approach, defined by a mean and standard deviation with 'a' ~ N(0.3 ± 0.15 a.u.), 'b' ~ N(10 ± 5 mmHg/a.u.), 'c' ~ N(35 ± 4 mmHg), 'd' ~ N(2.5 ± 0.5 a.u.), 's' ~ N(1 ± 0.5 a.u.).

2.3.3. Statistical analysis

To compare the goodness of fit of the models to the data, the Bayesian information criterion (BIC) was calculated for all the models based on Eq. (3) (Schwarz, 1978).

$$BIC = n \cdot \log\left(\frac{RSS}{n}\right) + K \cdot \log(n) \tag{3}$$

In the calculation of the BIC, n is the number of data points, RSS is the residual sum of squares error, and K is the number of model parameters. Here a lower BIC value indicates a closer fit to the true model and favours model simplicity (fewer parameters) to avoid overfitting.

3. Results

All 11 participants completed the full protocol. A few participants reported noticing a slight difference in smell/taste and feelings of breathlessness during the protocol, notably especially during the 40 s of 10 % CO_2 gas mixture. None-the-less, all participants responded that they would still be comfortable to repeat the study.

The TCD blood velocity measure and CO_2 trace for a representative subject is shown in Fig. 2. The rolling mean blood velocity signal, MCA$\underline{v}$, is overlaid on the TCD signal, and the $PETCO_2$ points and interpolation are overlaid on the CO_2 signal.

The range in $PETCO_2$ throughout the ramp protocol varied somewhat between subjects due to differences in the seal of the mask, breathing rate and depth as well as individual metabolism. On average, the maximum and minimum $PETCO_2$ values reached were 52 ± 2 mmHg and 27 ± 4 mmHg respectively, with a mean $PETCO_2$ span of 26 ± 4 mmHg. The average baseline $PETCO_2$ was 34 ± 2 mmHg. The average baseline MCA$\underline{v}$ was 32 ± 7 cm/s, and across all participants, the average MCA$\underline{v}$ reduction during hypocapnia was 71 ± 15 % of baseline and the subsequent increase during hypercapnia was 150 ± 23 % relative to baseline.

The MCA$\underline{v}$ is plotted as a function of the $PETCO_2$ for each participant,

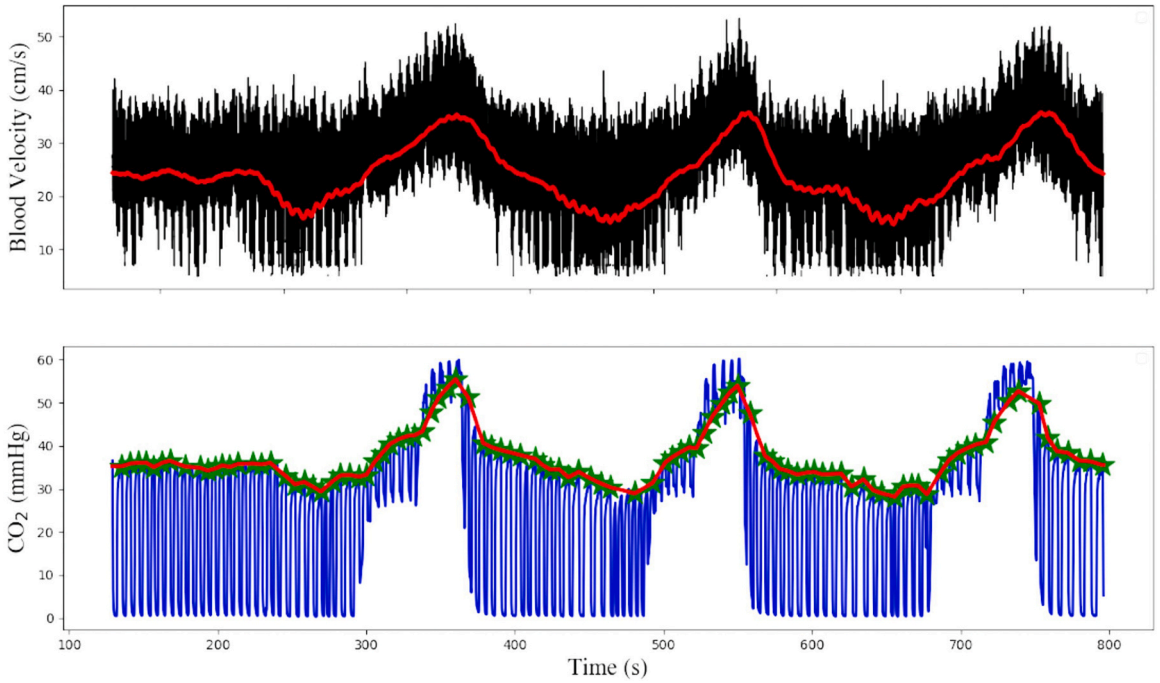

Fig. 2. TCD blood velocity (black, top) and CO_2 trace (blue, bottom) during the ramp protocol for a representative subject. The rolling mean of the blood flow velocity is overlaid in red (top). The end-tidal CO_2 points are represented by green stars and the interpolation between those points is shown in red (bottom). Sub-007.

presented in Fig. 3, including the linear regression lines, and the 4-parameter (4p) and 5-parameter (5p) models both fit with the LSR and Bayesian methods. It should be noted that subject 8 illustrated a highly variable $PETCO_2$ trace, attributed to shallow breathing.

Bar graphs of the parameter values for each subject for the 4p and 5p models are presented in Fig. 4 and Fig. 5 respectively. The values derived using the LSR and Bayes methods are presented for both models.

The BIC values of the linear, 4p LSR, 4p Bayes, 5p LSR, and 5p Bayes models are presented for each subject in Table 1. The subject mean and standard deviations (with and without sub-008) are also shown. Note that a more negative BIC value corresponds to a closer fit to the data, while accounting for the number of parameters in the model.

4. Discussion

In this work we present a $PETCO_2$ ramp protocol that allows the assessment of non-linear features of CVR with TCD. All 11 participants completed the protocol without complications, however 3 participants noted that breathing the air with 10 % CO_2 made them feel breathless.

The timing of the ramp protocol components was determined experimentally with 4 trained volunteers with the aim to find a balance between the largest feasible range in $PETCO_2$ while maintaining the safety and comfort of participants. The 5 deep breaths were chosen to decrease and briefly maintain a $PETCO_2$ below baseline. After 30 s of normal breathing on air, participants' $PETCO_2$ had returned to baseline, and after 40 s of breathing 5 % CO_2, the $PETCO_2$ values plateaued again at approximately 25 % above baseline. The 10 % CO_2 was maintained for the duration that all testing participants still found comfortable which resulted in a further increase in $PETCO_2$ to approximately 50 % above baseline.

The data showed minimal differences between the three ramp up segments with each acquisition except for in 1 participant (sub-008). The variation between the ramps in this participant is attributed to shallow breathing, resulting in $PETCO_2$ calculations from only partially expired breaths and significant differences in the $PETCO_2$ values between ramps. Due to potential inaccuracy of the $PETCO_2$ measurements, this participant was excluded from further statistical analysis. Noticeable differences between participant's MCA$\underline{v}$ responses to the ramp $PETCO_2$ protocol are that some participants show significantly more shouldering at the top and bottom of their response curve than others (such as sub-002, sub-010, and sub-006). The more linear responses (such as sub-003 and sub-004) could be due to not exceeding the linear regime for these participants. Furthermore, sub-002 with low resting blood flow measures had a large and fast increase in the normalised MCA$\underline{v}$ as $PETCO_2$ increased, but a minimal reduction in blood flow during the deep breaths. These features will be important to explore in larger participant groups as well as between sessions of repeated measurements on the same subject.

Non-linear CVR features were observed in the TCD data of all subjects, however some illustrate greater plateauing than others at the top or bottom ranges of the stimuli. The 4p and 5p models showed much closer fits to the data compared to a linear fit, based on significantly better BIC values for the non-linear models. Our results indicate that the linear regime in the CVR response is highly variable between subjects, as some individuals exhibit significant non-linear transitions or plateaus in the vascular response curve. These findings align with previous studies showing a sigmoidal CVR response as well as with literature showing that linear CVR metrics can be inconsistent due to variability in vascular reactivity across populations and experimental conditions (Battisti-Charbonney et al., 2011; Bhogal et al., 2014; Claassen et al., 2007; Ringelstein et al., 1988; Zhao et al., 2022). The sigmoidal modelling approach used in this study addresses these limitations by providing parameters that capture the non-linear dynamics of vascular reactivity, such as the slope, response span, and inflection point while still allowing for a linear regime to exist, which are critical for understanding individualized vascular responses.

Both LSR and Bayesian methods were used to fit the non-linear models, with the greatest difference in methodology being the incorporation of priors into the Bayesian approach. The gaussian priors were based on the expected behaviour of the healthy physiology and were informed by existing but limited research. All priors were given wide gaussian standard deviations as not to over-bias the fitting based on

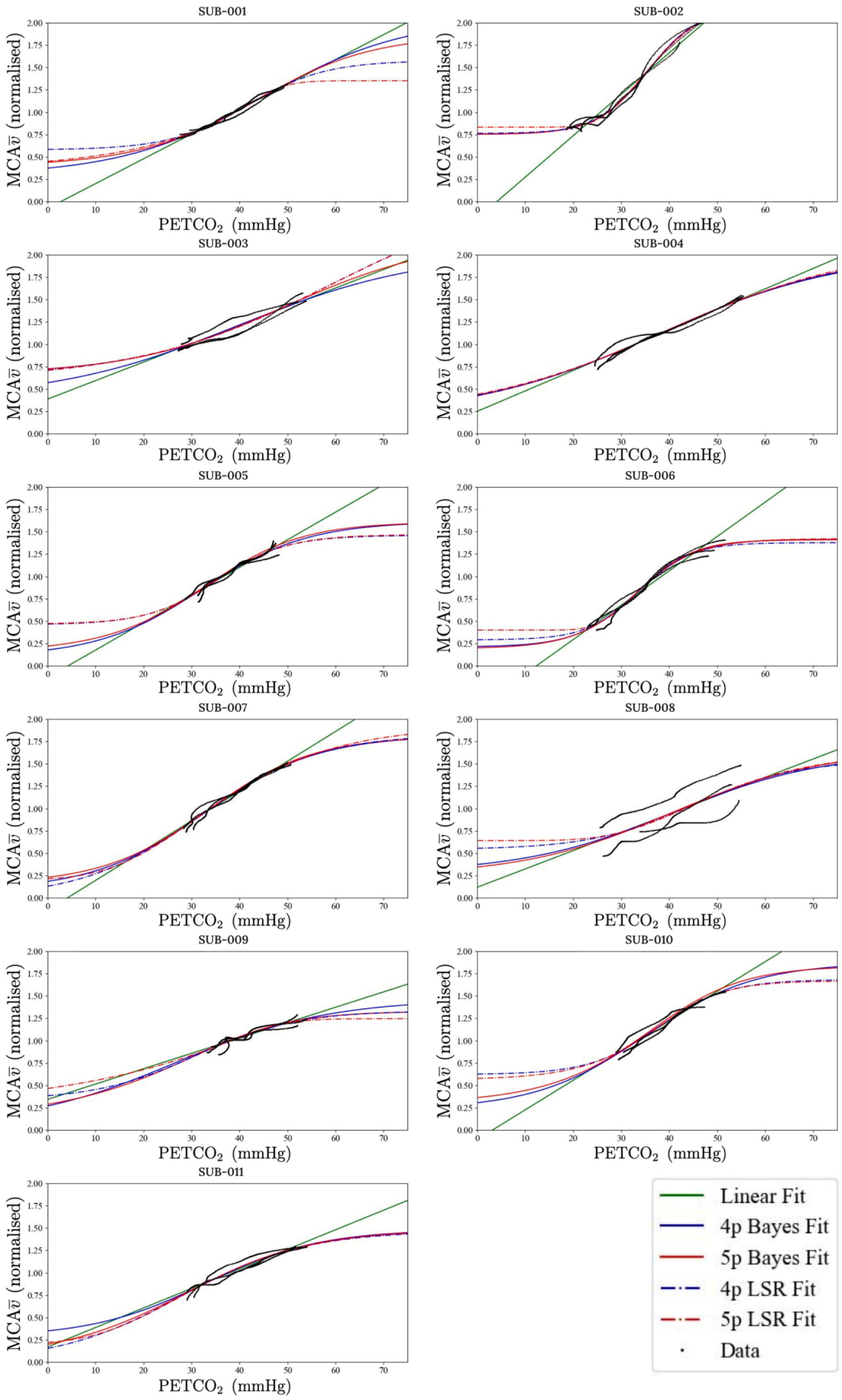

Fig. 3. MCA rolling-mean blood velocity as a function of $PETCO_2$ (black dots) for all subjects. Each dataset is fit with 2 models each with 2 fits: 4p LSR (blue, dashed line), 4p Bayes (blue, solid line), 5p LSR (red, dashed line), and 5p Bayes (red, solid line). Sub-011 was excluded due to noise and high variability.

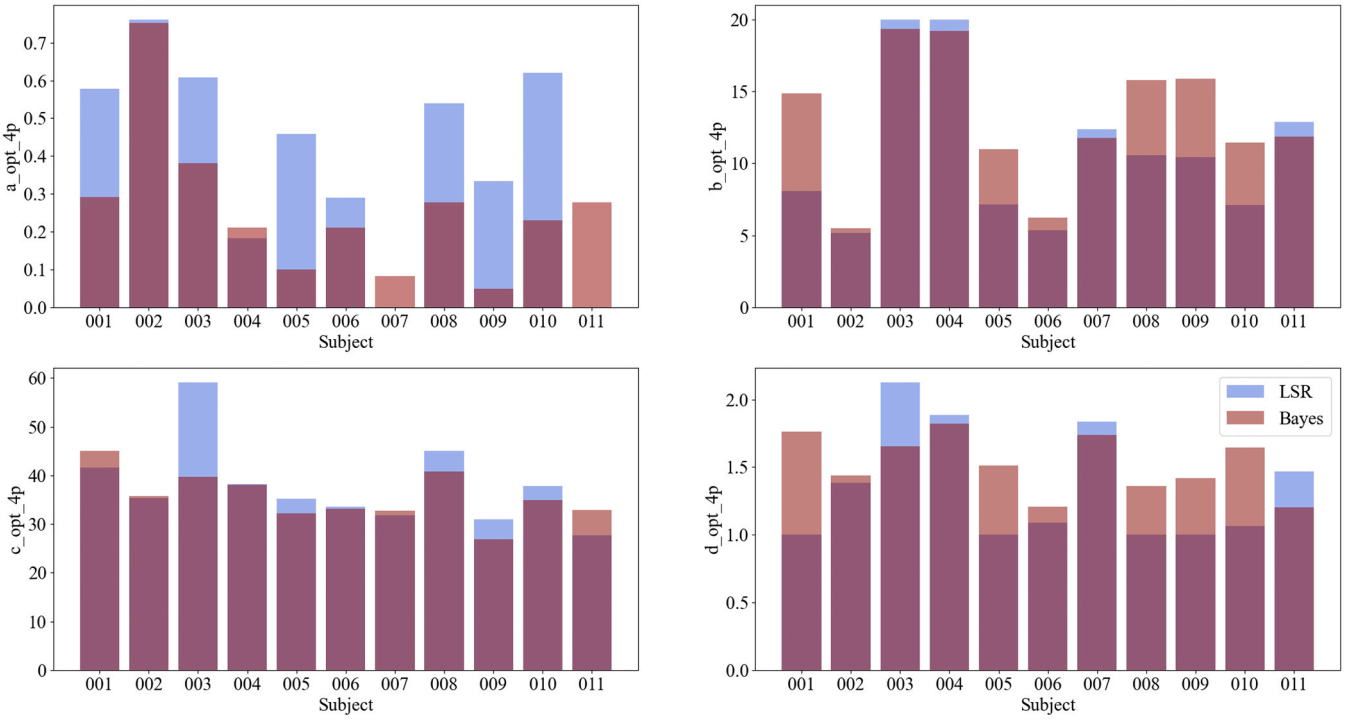

Fig. 4. 4-parameter model bar graphs for parameters a (lower plateau, top left), b (upper plateau, top right), c (inflection point, bottom left), and d (steepness, bottom right) for each subject fit with the LSR (blue) and Bayes (red) methods.

expectations and allow for variation between subjects. While there is limited research that clearly defines the normal boundaries of blood flow parameters in the MCA, assumptions were made based on other CVR and physiology studies. CBF below 50 % of baseline has been shown to be a lower limit in the conscious brain and is very unlikely to occur, so while the absolute lower bounds of the sigmoid (parameter a) were set at 0, the priors for the Bayesian modelling of the lower bound were set at 30 % of baseline (Claassen et al., 2021; del Zoppo et al., 2011). Furthermore, based on the results of non-linear CVR mapping by Fan et al. and Ringelstein et al., it was assumed that the MCA$\underline{v}$ was unlikely to ever go above 300 % of baseline and the upper shoulder regime of the sigmoid occurred between 130 % and 160 % for most adults (Ringelstein et al., 1988; Fan et al., 2016). As a result, the maximum span of the sigmoid (parameter d) was set to reflect no more than a 4-fold increase in blood flow from hypocapnia and the priors for the Bayesian analysis were set to represent a 250 % increase with a wide standard deviation of $\pm$ 50 %. The bounds for the slope of the linear regime (parameter b), inflection point (parameter c), and asymmetry parameter (parameter s), were all set to have wide bounds, with the slope assumed to be positive, and the priors of the inflection point set with a mean of 35 mmHg based on previous CVR research (Battisti-Charbonney et al., 2011; Bhogal et al., 2014; Claassen et al., 2007; Fan et al., 2016).

When assessed using the Bayesian fitting, the parameters values for the 4p and 5p models are very similar, however with the LSR fit, the values of the inflection point (parameter b) trades off significantly with the asymmetry parameter (parameter s) in the 5p model. The asymmetry parameter also showed significant variation between subjects when fit with the LSR method and despite resulting in the same BIC score (BIC = $-$4035 for both the LSR 4p and 5p methods), this suggests the model is overfitting the data. When fitted with the Bayesian method, the asymmetry parameter stayed close to s = 1 for all subjects, suggesting that the sigmoids are quite symmetrical. With the minor asymmetry parameters, the 5p model still showed a slightly worse BIC score of $-$3994 compared to $-$4022 for the Bayes 4p model.

The Bayesian and LSR methods showed noticeable differences between the parameter values for some, but not all subjects, especially for the minimum blood velocity (parameter a), with more minor differences between the other parameters. When assessed using both methods, the parameter ‘c’, representing the inflection point, aligns with previous literature where sigmoid midpoints typically sit between 36 and 46 mmHg, slightly above resting $PETCO_2$ levels (Battisti-Charbonney et al., 2011; Claassen et al., 2007; Fan et al., 2016). Similarly, the response range (‘a’ and ‘d’) is consistent with reported spans, ranging from 90 % to 150 % change in MCAv in TCD, but is more variable when assessed using the LSR method compared to the Bayesian method (Claassen et al., 2007; Fan et al., 2016). Our results suggest that the range of the linear regime is variable between participants, in some cases showing a linear regime above 10 mmHg which is higher than previously reported (Battisti-Charbonney et al., 2011; Bhogal et al., 2014; Fan et al., 2016). With the advantage of the priors, the Bayesian method more closely approaches the expected physiological ranges, while the LSR method hits the parameter limits for a number of participants in which cases it goes to unreasonable extremes to more closely fit all of the data, such as in the case of some very high asymmetry values with the 5p model. While the LSR method achieves a lower BIC score, this advantage is inherent to its optimization process, which explicitly minimizes the residual sum of squares error, a key component in BIC calculation. In contrast, the Bayesian approach is not directly optimized for this criterion, introducing a bias in favour of the LSR method when evaluated using the BIC. None-the-less, it is important to note that despite fitting the data as well as the physiological priors, the Bayesian method still results in a goodness of fit comparable to the LSR method, with a BIC of $-$4022 for the Bayesian 4p method and $-$4035 for the LSR 4p method.

It is important to note that neither method can be declared definitively more accurate or unbiased in the absence of a ’gold standard’ or simulation-based validation. Instead, each approach offers unique advantages: the LSR method excels in computational simplicity and direct optimization of residuals, whereas the Bayesian approach incorporates prior information and generates posterior distributions, enabling richer parameter estimation and uncertainty quantification.

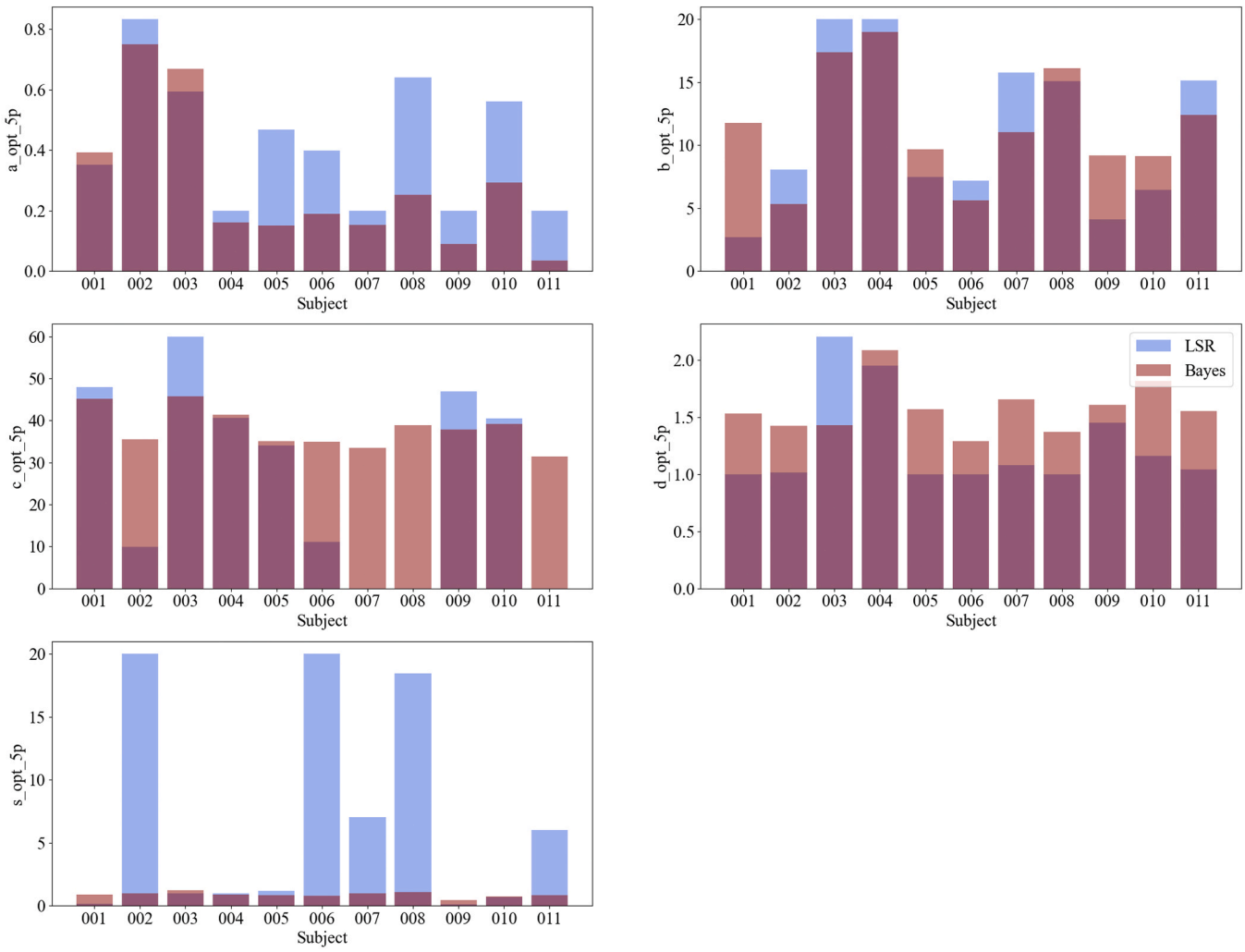

Fig. 5. 5-parameter model bar graphs for parameters a (lower plateau, top left), b (upper plateau, top right), c (inflection point, middle left), d (steepness, middle right), and s (symmetry, bottom left) for each subject fit with the LSR (blue) and Bayes (red) methods.

Table 1
Bayesian information criterion error for linear regression, 4p LSR, 4p Bayes, 5p LSR, and 5p Bayes for all subjects including the mean and standard deviation for each model across subjects, with and without sub-008.

Subject	Linear	LSR 4p	LSR 5p	Bayes 4p	Bayes 5p
Sub−001	−4536	−4673	−4678	−4628	−4636
Sub−002	−3159	−3775	−3806	−3767	−3766
Sub−003	−3733	−3747	−3740	−3717	−3736
Sub−004	−4144	−4098	−4091	−4095	−4089
Sub−005	−4270	−4321	−4315	−4313	−4203
Sub−006	−3447	−3751	−3755	−3740	−3725
Sub−007	−4003	−4074	−4070	−4073	−4022
Sub−008	*−2008*	*−2000*	*−1994*	*−1997*	*−1989*
Sub−009	−3930	−3979	−3974	−3969	−3955
Sub−010	−3912	−3946	−3940	−3938	−3833
Sub−011	−3910	−3987	−3981	−3979	−3977
Mean±SD	***−3732***	***−3850***	***−3849***	***−3838***	***−3812***
	±683	***±671***	***±672***	***±666***	***±659***
Mean ±SD	**−3904**	**−4035**	**−4035**	**−4022**	**−3994**
*	**±394**	**±287**	**±285**	**±281**	**±276**

* with sub-008 removed

4.1. Limitations and future work

With TCD allowing for high-temporal resolution blood velocity measures at a low cost, it is routinely used in clinical practice and research, however it is not without its limitations. The blood velocity measure can be affected by the angle of the probe with the blood vessel and a TCD's accuracy is highly dependent on the operator (Purkayastha and Sorond, 2013). To mitigate these risks, the same trained operator helped with the acquisition of all TCD data, and MCA$\underline{v}$ values were normalised relative to the MCA$\underline{v}$ measured at baseline. Furthermore, since our CVR metrics were only based on blood velocity measured in the MCA it is not necessarily representative of blood flow in the rest of the brain as there may exist regional differences (Battisti-Charbonney et al., 2011; Kety and Schmidt, 1948; Willie et al., 2012). For example, integrating multimodal validation with BOLD fMRI would provide an opportunity to enrich our understanding of cerebrovascular dynamics across the brain. While TCD measures reflect blood velocity changes within the MCA, BOLD fMRI captures oxygenation-dependent signal changes that also incorporates cerebral perfusion and metabolism with high spatial resolution. Future assessment of this CVR ramp protocol in MRI will allow for measures of cerebral blood flow with high spatial resolution and the study of regional CVR across the brain.

One of the major assumptions in many CVR studies, including our own, is the reliance on $PETCO_2$ as a surrogate measure for $PaCO_2$. While $PETCO_2$ is a non-invasive and easily obtainable measure, it may not always accurately reflect $PaCO_2$ as it can be influenced by variance in ventilation and perfusion (Bussotti et al., 2008; Sun et al., 2022; Thirapatarapong et al., 2013; Wasserman et al., 1967). Consequently, the use of $PETCO_2$ as a proxy for $PaCO_2$, while practical and frequently

implemented in CVR studies, introduces a degree of uncertainty and potential error in the CVR values (Nassar and Schmidt, 2017). Furthermore, other studies using programmable gas delivery systems can offer significant improvements in the stability of $PETCO_2$ values compared to fixed inspired CO_2 methods, and can therefore reduce the potential for error and enhance the precision of CVR mapping (Blockley et al., 2011; Fisher et al., 2016; Robbins et al., 1982; Wise et al., 2007). Moreover, direct arterial measurements, although more invasive, provide the most accurate assessment of $PaCO_2$. Our study utilises a fixed inhaled CO_2 system and breathing protocol, which, although less precise, is inexpensive and very easy to implement, making it a practical option for larger-scale or resource-limited studies.

Another limitation in our study is that continuous arterial blood pressure (ABP) measurements were not taken throughout the ramp protocol and only a baseline blood pressure measure was acquired while the participants were at rest using an arm cuff to rule out hypertension. Continuous ABP measurements could provide more insights into CVR by means of a conductance index which can somewhat account for the impact of changes in perfusion pressure on blood velocity and vasodilation (Bailey et al., 2022; Miller et al., 2018). Some studies have demonstrated that changes in ABP induced by vasoactive stimuli can impact the CBF response and therefore affect the CVR values in some adults (Willie et al., 2012; Howe et al., 2020; Regan et al., 2014; Walsh et al., 2024). Other studies have shown that when using up to 7 % inspired CO_2 gas mixtures, the increase in ABP has minimal effects on MCAv and CVR (Worley et al., 2024). Further research by Battisti-Charbonney et al. showed that the MCAv response to CO_2 was unchanged by ABP considerations up to a threshold of ~50 mmHg, above which both MCAv and ABP demonstrated a linear increase with CO_2 tension (Battisti-Charbonney et al., 2011). A linear regime in MCA$\underline{v}$ was not noticeable at high $PETCO_2$ values in the results of our study, however the maximum $PETCO_2$ reached by most participants was only slightly above 50 mmHg (52 ± 2 mmHg on average) and was only maintained for a few seconds before participants returned to breathing air. It should also be noted that in patient groups, ABP could more significantly alter CVR (Dumville et al., 1998), and accounting for ABP may become increasingly important when assessing older adults (Miller et al., 2018). Future studies may benefit from measuring and accounting for continuous ABP changes especially when using hypercapnic stimuli that go significantly above 50 mmHg or when investigating patient groups.

It should also be noted that the model bounds and priors presented in our analysis of the CVR curves are based on a limited body of research on the physiological bounds of cerebral blood flow in nominally healthy humans. To mitigate this, large absolute bounds and wide standard deviations in the gaussian priors of the Bayesian models were defined to allow for subject variability and to not overly bias the model fits. Furthermore, the use of the BIC to compare models was presented as a means of assessing the distance of the model fits from the data, however it is not a fair direct comparison between the Bayesian and LSR modelling approaches since the BIC is based on the residual sum of squares error which the LSR method utilises to define its fit. Future analyses would benefit from including other statistical comparisons to assessment of model fits such as using separate datasets for model fitting and validation, or by leveraging simulations to benchmark the accuracy and bias of each approach under controlled conditions. Additionally, while this study focused on the dilation phase of the CVR response, future research could investigate the constriction phase to provide a more comprehensive assessment of cerebrovascular dynamics. The potentially differing physiological mechanisms of dilation and constriction warrant further exploration.

While our ramp protocol and models provide valuable insights into the normal functioning of cerebrovascular mechanisms, it has limitations when applied to pathological conditions. Non-linear CVR is an emerging area of study that may offer a deeper understanding of cerebrovascular health and disease. However, the applicability of our findings to pathological states remains uncertain due to the lack of extensive research in this area, especially when using Bayesian priors based on physiology of healthy adults, as different models may be needed in diseased states. Studies have indicated that non-linear CVR measures can reveal important differences in patients with cerebrovascular diseases. For instance, research on patients with moyamoya disease has shown altered CVR patterns, suggesting potential diagnostic and prognostic utility (Deckers et al., 2021; He et al., 2024; Liu et al., 2021; Sam et al., 2015). Similarly, other studies have identified changes in CVR in conditions such as stroke, cognitive decline, and traumatic brain injury, highlighting its relevance in various pathologies (Churchill et al., 2020; da Costa et al., 2016; Krainik et al., 2005; Markus and Cullinane, 2001; Mutch et al., 2016; Aslanyan et al., 2024). These findings imply that CVR measures could be useful in distinguishing and better understanding cerebrovascular pathology, and non-linear CVR may offer additional insights into the nature of the CVR impairment. Nevertheless, more research is needed to better understand how non-linear CVR changes in different diseases and to establish standardised protocols for its assessment in clinical settings. Expanding the study of non-linear CVR to pathological cohorts will be essential to validate its clinical applicability and enhance our understanding of cerebrovascular changes in disease.

Finally, our study presents the ramp protocol in only a small sample size of 11 healthy adults and requires more research in a larger cohort with a greater diversity of ages, backgrounds, and lifestyle factors to assess population variability, protocol tolerance, and repeatability. With the large dynamic range in blood flow, ease of implementation, high completion rate, and low equipment cost compared to other methods of assessing CVR, these methods and models could offer an accurate and convenient quantification of CBF dynamics useful for clinical adoption.

5. Conclusion

We developed a low-cost, clinically relevant method for assessing the non-linear features of CVR with TCD based on a $PETCO_2$ ramp protocol. This novel CVR protocol is designed as an accessible entryway into the study of non-linear CVR dynamics. The CVR responses to this protocol were better fit with 4- and 5-parameter sigmoids than a linear model and Bayesian model fitting allowed for prior physiological information to favour fitting the data within reasonable bounds. Future work includes extending the use of this cost-effective ramp protocol and non-linear CVR modelling in MRI in a larger participant group.

Funding acknowledgements

This work was supported by Engineering and Physical Sciences Research Council UK through grant EP/S021507/1. GH was supported by Clarendon, and SS by the Rhodes Trust and the Canadian Institutes of Health Research (DSG-193252).

Author contribution statement

GH contributed to the study concept and design, recruitment, and led the data acquisition, analysis and interpretation, and writing of the manuscript. SS contributed to data acquisition, recruitment, and critical revision of the manuscript. JP contributed to ethics approvals, study design, data acquisition, and critical revision of the manuscript. DPB developed the original study concept and design, and contributed to critical revision of the manuscript, and study supervision. All authors read and approved the final manuscript.

CRediT authorship contribution statement

Bulte Daniel P.: Writing – review & editing, Supervision, Methodology, Investigation, Funding acquisition, Conceptualization. **Pinto Joana:** Writing – review & editing, Project administration,

Methodology, Funding acquisition, Data curation. **Sparks Sierra:** Writing – review & editing, Project administration, Data curation. **Hayes Genevieve:** Writing – review & editing, Writing – original draft, Visualization, Validation, Software, Project administration, Methodology, Investigation, Formal analysis, Data curation, Conceptualization.

Declaration of Competing Interest

The authors declare that the research was conducted in the absence of any commercial or financial relationships that could be construed as a potential conflict of interest.

Acknowledgements

The authors would like to thank all the volunteers who participated in this study and Dr. Johannes Klein for training the team on transcranial Doppler ultrasound.

Data availability

Data will be made available on request.

References

Aslanyan, V., Mack, W.J., Ortega, N.E., et al., 2024. Cerebrovascular reactivity in Alzheimer's disease signature regions is associated with mild cognitive impairment in adults with hypertension. Alzheimers Dement 20, 1784–1796.
Bailey, T.G., Klein, T., Meneses, A.L., et al., 2022. Cerebrovascular function and its association with systemic artery function and stiffness in older adults with and without mild cognitive impairment. Eur. J. Appl. Physiol. 122, 1843–1856.
Battisti-Charbonney, A., Fisher, J., Duffin, J., 2011. The cerebrovascular response to carbon dioxide in humans. J. Physiol. 589, 3039–3048.
Bhogal, A.A., Philippens, M.E.P., Siero, J.C.W., et al., 2015. Examining the regional and cerebral depth-dependent BOLD cerebrovascular reactivity response at 7T. NeuroImage 114, 239–248.
Bhogal, A.A., Siero, J.C.W., Fisher, J.A., et al., 2014. Investigating the non-linearity of the BOLD cerebrovascular reactivity response to targeted hypo/hypercapnia at 7T. NeuroImage 98, 296–305.
Blockley, N.P., Driver, I.D., Francis, S.T., et al., 2011. An improved method for acquiring cerebrovascular reactivity maps. Magn. Reson Med. 65, 1278–1286.
Bright, M.G., Murphy, K., 2013. Reliable quantification of BOLD fMRI cerebrovascular reactivity despite poor breath-hold performance. NeuroImage 83, 559–568.
Burley, C.V., Francis, S.T., Thomas, K.N., et al., 2021. Contrasting measures of cerebrovascular reactivity between mri and doppler: a cross-sectional study of younger and older healthy individuals (Epub ahead of print). Front. Physiol. 12. https://doi.org/10.3389/fphys.2021.656746.
Bussotti, M., Magrì, D., Previtali, E., et al., 2008. End-tidal pressure of CO2 and exercise performance in healthy subjects. Eur. J. Appl. Physiol. 103, 727–732.
Churchill, N.W., Hutchison, M.G., Graham, S.J., et al., 2020. Cerebrovascular reactivity after sport concussion: from acute injury to 1 year after medical clearance. Front. Neurol. 11. ⟨https://www.frontiersin.org/articles/10.3389/fneur.2020.00558⟩. accessed 10 July 2023).
Claassen, J.A.H.R., Thijssen, D.H.J., Panerai, R.B., et al., 2021. Regulation of cerebral blood flow in humans: physiology and clinical implications of autoregulation. Physiol. Rev. 101, 1487–1559.
Claassen, J.A.H.R., Zhang, R., Fu, Q., et al., 2007. Transcranial Doppler estimation of cerebral blood flow and cerebrovascular conductance during modified rebreathing. J. Appl. Physiol. 102, 870–877.
da Costa, L., van Niftrik, C.B., Crane, D., et al., 2016. Temporal profile of cerebrovascular reactivity impairment, gray matter volumes, and persistent symptoms after mild traumatic head injury. Front. Neurol. 7, 70.
Deckers, P.T., Hoek, W., Kronenburg, A., et al., 2021. Contralateral improvement of cerebrovascular reactivity and TIA frequency after unilateral revascularization surgery in moyamoya vasculopathy. NeuroImage Clin. 30, 102684.
van der Zande, F.H.R., Hofman, P. a M., Backes, W.H., 2005. Mapping hypercapnia-induced cerebrovascular reactivity using BOLD MRI. Neuroradiology 47, 114–120.
Duffin, J., Sobczyk, O., Crawley, A., et al., 2017. The role of vascular resistance in BOLD responses to progressive hypercapnia. Hum. Brain Mapp. 38, 5590–5602.
Dumville, J., Panerai, R.B., Lennard, N.S., et al., 1998. Can cerebrovascular reactivity be assessed without measuring blood pressure in patients with carotid artery disease? Stroke 29, 968–974.
EODG. Oxford Physics: Atmospheric, Oceanic and Planetary Physics: Weather, ⟨https://eodg.atm.ox.ac.uk/eodg/weather/weather_nocol.html⟩.
Fan, J.-L., Subudhi, A.W., Duffin, J., et al., 2016. AltitudeOmics: resetting of cerebrovascular CO2 reactivity following acclimatization to high altitude. Front. Physiol. 6. ⟨https://www.frontiersin.org/journals/physiology/articles/10.3389/fphys.2015.00394⟩. accessed 7 March 2024).
Fisher, J.A., Iscoe, S., Duffin, J., 2016. Sequential gas delivery provides precise control of alveolar gas exchange. Respir. Physiol. Neurobiol. 225, 60–69.
Fisher, J.A., Sobczyk, O., Crawley, A., et al., 2017. Assessing cerebrovascular reactivity by the pattern of response to progressive hypercapnia. Hum. Brain Mapp. 38, 3415–3427.
He, S., Wang, X., Niu, H., et al., 2024. Evaluation of cerebrovascular reactivity in moyamoya disease using oxygen-dependent magnetic resonance imaging. iScience 27, 108923.
Howe, C.A., Caldwell, H.G., Carr, J., et al., 2020. Cerebrovascular reactivity to carbon dioxide is not influenced by variability in the ventilatory sensitivity to carbon dioxide. Exp. Physiol. 105, 904–915.
Kester, D., Mueller, M., 2021. BayesicFitting, a PYTHON toolbox for Bayesian fitting and evidence calculation.: including a Nested Sampling implementation. Astron Comput. 37, 100503.
Kety, S.S., Schmidt, C.F., 1948. The effects of altered arterial tensions of carbon dioxide and oxygen on cerebral blood flow and cerebral oxygen consumption of normal young men 1. J. Clin. Invest 27, 484–492.
Krainik, A., Hund-Georgiadis, M., Zysset, S., et al., 2005. Regional impairment of cerebrovascular reactivity and BOLD signal in adults after stroke. Stroke 36, 1146–1152.
Liu, P., Liu, G., Pinho, M.C., et al., 2021. Cerebrovascular reactivity mapping using resting-state BOLD functional mri in healthy adults and patients with Moyamoya Disease. Radiology 299, 419–425.
Liu, P., Xu, C., Lin, Z., et al., 2020. Cerebrovascular reactivity mapping using intermittent breath modulation. NeuroImage 215, 116787.
Markus, H., Cullinane, M., 2001. Severely impaired cerebrovascular reactivity predicts stroke and TIA risk in patients with carotid artery stenosis and occlusion. Brain J. Neurol. 124, 457–467.
McDonnell, M.N., Berry, N.M., Cutting, M.A., et al., 2013. Transcranial Doppler ultrasound to assess cerebrovascular reactivity: reliability, reproducibility and effect of posture. PeerJ 1, e65.
Miller, K.B., Howery, A.J., Harvey, R.E., 2018. Cerebrovascular reactivity and central arterial stiffness in habitually exercising healthy adults. Front. Physiol. 9. https://doi.org/10.3389/fphys.2018.01096. Epub ahead of print 17 August.
Mutch, W.A.C., Ellis, M.J., Ryner, L.N., et al., 2016. Brain magnetic resonance imaging CO2 stress testing in adolescent postconcussion syndrome. J. Neurosurg. 125, 648–660.
Nassar, B.S., Schmidt, G.A., 2017. Estimating arterial partial pressure of carbon dioxide in ventilated patients: how valid are surrogate measures? Ann. Am. Thorac. Soc. 14, 1005–1014.
Pinto, J., Bright, M.G., Bulte, D.P., et al., 2021. Cerebrovascular reactivity mapping without gas challenges: a methodological guide (Epub ahead of print). Front. Physiol. 11.
Purkayastha, S., Sorond, F., 2013. Transcranial doppler ultrasound: technique and application. Semin Neurol. 32, 411–420.
Regan, R.E., Fisher, J.A., Duffin, J., 2014. Factors affecting the determination of cerebrovascular reactivity. Brain Behav. 4, 775–788.
Ringelstein, E.B., Sievers, C., Ecker, S., et al., 1988. Noninvasive assessment of CO2-induced cerebral vasomotor response in normal individuals and patients with internal carotid artery occlusions. Stroke 19, 963–969.
Ringelstein, E.B., Van Eyck, S., Mertens, I., 1992. Evaluation of cerebral vasomotor reactivity by various vasodilating Stimuli: comparison of CO2 to acetazolamide. J. Cereb. Blood Flow. Metab. 12, 162–168.
Robbins, P.A., Swanson, G.D., Howson, M.G., 1982. A prediction-correction scheme for forcing alveolar gases along certain time courses. J. Appl. Physiol. 52, 1353–1357.
Sam, K., Poublanc, J., Sobczyk, O., et al., 2015. Assessing the effect of unilateral cerebral revascularisation on the vascular reactivity of the non-intervened hemisphere: a retrospective observational study. BMJ Open 5, e006014.
Schwarz, G., 1978. Estimating the dimension of a model. Ann. Stat. 6, 461–464.
Sleight, E., Stringer, M.S., Marshall, I., et al., 2021. Cerebrovascular reactivity measurement using magnetic resonance imaging: a systematic review. Front. Physiol. 12. ⟨https://www.frontiersin.org/articles/10.3389/fphys.2021.643468⟩. accessed 1 December 2022).
Sobczyk, O., Battisti-Charbonney, A., Fierstra, J., et al., 2014. A conceptual model for CO2-induced redistribution of cerebral blood flow with experimental confirmation using BOLD MRI. NeuroImage 92, 56–68.
Sparks, S., Hayes, G., Pinto, J., et al., 2024. Characterising cerebrovascular reactivity and the pupillary light response–a comparative study. Epub ahead of print 8 August Front. Physiol. 15. https://doi.org/10.3389/fphys.2024.1384113.
Sun, X., Shi, X., Cao, Y., et al., 2022. Variation of PetCO2 during incremental exercise and severity of IPAH and CTEPH. BMC Pulm. Med. 22, 249.
The pandas development team. pandas-dev/pandas: Pandas. Epub ahead of print 20 September 2024. DOI: 10.5281/zenodo.13819579.
Thirapatarapong, W., Armstrong, H.F., Thomashow, B.M., et al., 2013. Differences in gas exchange between severities of chronic obstructive pulmonary disease. Respir. Physiol. Neurobiol. 186, 81–86.
Virtanen, P., Gommers, R., Oliphant, T.E., et al., 2020. SciPy 1.0: fundamental algorithms for scientific computing in Python. Nat. Methods 17, 261–272.
Walsh, H.J., Junejo, R.T., Lip, G.Y.H., et al., 2024. The effect of hypertension on cerebrovascular carbon dioxide reactivity in atrial fibrillation patients. Hypertens. Res. 47, 1678–1687.
Wasserman, K., Van Kessel, A.L., Burton, G.G., 1967. Interaction of physiological mechanisms during exercise. J. Appl. Physiol. 22, 71–85.
Willie, C.K., Macleod, D.B., Shaw, A.D., et al., 2012. Regional brain blood flow in man during acute changes in arterial blood gases. J. Physiol. 590, 3261–3275.
Wise, R.G., Pattinson, K.T.S., Bulte, D.P., et al., 2007. Dynamic forcing of end-tidal carbon dioxide and oxygen applied to functional magnetic resonance imaging. J. Cereb. Blood Flow. Metab. J. Int. Soc. Cereb. Blood Flow. Metab. 27, 1521–1532.

Worley, M.L., Reed, E.L., Klaes, N., et al., 2024. Cool head-out water immersion does not alter cerebrovascular reactivity to hypercapnia despite elevated middle cerebral artery blood velocity: a pilot study. PLoS One 19, e0298587.
Zhao, M.Y., Woodward, A., Fan, A.P., et al., 2022. Reproducibility of cerebrovascular reactivity measurements: a systematic review of neuroimaging techniques*. J. Cereb. Blood Flow. Metab. 42, 700–717.
Zheng, Y., Pan, Y., Harris, S., et al., 2010. A dynamic model of neurovascular coupling: implications for blood vessel dilation and constriction. NeuroImage 52, 1135–1147.
del Zoppo, G.J., Sharp, F.R., Heiss, W.-D., et al., 2011. Heterogeneity in the penumbra. J. Cereb. Blood Flow. Metab. 31, 1836–1851.